Available online at www.sciencedirect.com

SciVerse ScienceDirect

Ceramics International 39 (2013) 3165–3171

CERAMICS INTERNATIONAL

www.elsevier.com/locate/ceramint

Influence of temperature on the morphology and photocatalytic activity of $ZnGa_2O_4$ crystallites prepared by hydrothermal method

Liangliang Liu, Jianfeng Huang*, Liyun Cao, Jianpeng Wu, Jie Fei, Haibo Ouyang, Chunyan Yao

Key Laboratory of Auxiliary Chemistry & Technology for, Light Chemical Industry of Ministry of Education, School of Materials Science and Engineering, Shaanxi University of Science and Technology, Xi'an, Shaanxi 710021, China

Received 5 July 2012; received in revised form 13 September 2012; accepted 28 September 2012
Available online 5 October 2012

Abstract

$ZnGa_2O_4$ crystallites were synthesized via a hydrothermal method in the temperature between 160 °C and 200 °C at the pH of 13.5 using $ZnSO_4 \cdot 10H_2O$ and Ga_2O_3 as source materials. The phase and microstructure of the as-prepared $ZnGa_2O_4$ crystallites were characterized by X-ray diffraction (XRD), scanning electron microscopy (SEM), and transmission electron microscopy (TEM). It is found that the nano-spheric $ZnGa_2O_4$ crystallites can be synthesized at the temperature of 160 °C, while the assembled three-dimensional structure of the $ZnGa_2O_4$ crystallites can be achieved at 170–200 °C. In addition, the growth mechanisms of nano-spheric and three-dimensional structure of the $ZnGa_2O_4$ crystallites are preliminarily discussed and it is found that the $ZnGa_2O_4$ nucleation rate was controlled by the formation of $Ga(OH)_4^-$. The photocatalytic activity of $ZnGa_2O_4$ crystallites was evaluated using Rhodamine B (RB) as a model pollutant. Results showed that the photocatalytic activity of the $ZnGa_2O_4$ crystallites can be significantly decreased and the areal activity of them are increased by increasing the temperature from 160 °C to 200 °C, which may be caused by the improved crystallization and a cuboid-like morphology. The best photodegradation efficiency was shown by the sample prepared at 160 °C and the degradation efficiency of Rhodamine B was 98.4% in 60 min.

Keywords: Hydrothermal method; $ZnGa_2O_4$ crystallites; Photocatalytic activity

1. Introduction

$ZnGa_2O_4$ is an important p-type semiconductor material with extensive application in flat panel display [1], thin film electroluminescence display [2] and vacuum florescent display [3]. Furthermore, on account of better chemical stability over sulfide phosphors, $ZnGa_2O_4$ can endure a high electron beam current [4]. Recently, due to its excellent performance in water splitting and air-pollution control, $ZnGa_2O_4$ has received considerable attention [5]. Dyes as one of the main types of pollutants in waste water are emphasized. Because $ZnGa_2O_4$ has hybridized orbitals of Ga4s4p, Zn4s4p and the wide band gap (4.4 eV), it can promote that the mobility of photogenerated electrons and the absorption efficiency in UV lamps are the most available light source for waste water purification [6]. Therefore, $ZnGa_2O_4$ may be more efficient in degrading dyes. In a series of earlier works, Hirano [7–9] drew the conclusion that single-phase $ZnGa_2O_4$ particles were synthesized from a mixed solution of gallium and zinc salts under hydrothermal conditions at 150–240 °C. But no result about the photocatalytic activity and the growth mechanism of $ZnGa_2O_4$ was reported. Wei [10] proved that $ZnGa_2O_4$ powder and thin film fabricated by sol–gel process had better photocatalytic performance in degradation of methylene blue. Compared to the sol–gel process, the hydrothermal technique is relatively convenient without later thermal treatment. Besides, its morphology can be controlled more easily. However, the Influence of processing parameter on the morphology and photocatalytic performance of $ZnGa_2O_4$ crystallites using hydrothermal process is rarely reported.

In the present work, $ZnGa_2O_4$ crystallites were synthesized by hydrothermal method by using gallium oxide (Ga_2O_3) as

*Corresponding author. Tel./fax: +86 29 86168803.
E-mail address: elite19880219@163.com (J. Huang).

0272-8842/$ - see front matter © 2012 Elsevier Ltd and Techna Group S.r.l. All rights reserved.
http://dx.doi.org/10.1016/j.ceramint.2012.09.101

gallium source. Rhodamine B(RB) was used as dye aqueous solution in the degradation test. The influence of hydrothermal temperature on the phase, morphology and photocatalytic performance of $ZnGa_2O_4$ crystallites are particularly investigated.

2. Experimental

2.1. Preparation of $ZnGa_2O_4$ crystallites

A typical synthesis route of $ZnGa_2O_4$ crystallites were as follows: first, 0.288 g $ZnSO_4 \cdot 10H_2O$(AR) and 0.187 g Ga_2O_3(AR) were dissolved in deionized water and stirred for 10 min to form a suspension. Then 2 mol/L NaOH(AR) was added to adjust the suspension pH value to 8–14 with continuous stirring. After 10 min of stirring, the mixture was poured into a 20 ml Teflon-lined stainless reactor with the volume filling ration of 67%, heated at 140–200 °C for 4 h, and then cooled down to room temperature naturally. The products were washed with deionized water and ethanol 3 times, respectively. Finally, they were dried in the oven at 80 °C for 3 h.

2.2. Characterization

The powder X-ray diffraction patterns of as-prepared samples were measured using an X-ray diffractometer (XRD, D/max-2200PC, Rigaku, Japan) with Cu K_α radiation at a scanning rate of $8^\circ\ min^{-1}$ in the 2θ range from 15° to 70°. The surface morphology was observed using a Scanning Electron Microscopy (SEM, JSM-6390A, JEOL, Japan). Transmission electron microscopy (TEM, JEM-3010, JEOL, Japan) was used to provide selected area electron diffraction (SAED) and high-resolution TEM (HRTEM) images of the powders. The specific surface area of the sample was measured using the Brunauer–Emmett–Teller (BET) method using Surface area and pore size Analyzer (SA3100, Beckman Coulter, America). Prior to the measurements, samples were degassed at 200 °C for 2 h.

2.3. Photocatalytic activity test

The photocatalytic degradation tests were carried out in photoreactor (BL-GHX-V, Shanghai) using 0.02 g $ZnGa_2O_4$ particles dispersed in 20 ml RB solution (10 mg/L). Before the reaction, the photocatalyst was soaked in RB solution with a dark environment for 30 min to achieve adsorption equilibrium of RB on the catalyst. The light source was a 300 W mercury lamp and continuous magnetic stirring should be kept to maintain the suspension of $ZnGa_2O_4$ particles in the RB solution. The reaction temperature was kept at 25 °C. Then 5 mL of the suspension was collected for every 15 min and centrifuged at 3500 rpm.The clear solution was separated from the above suspension and the RB concentration was measured by an Ultraviolet-visible Spectrophotometer (UV-2550, Shanghai, China).

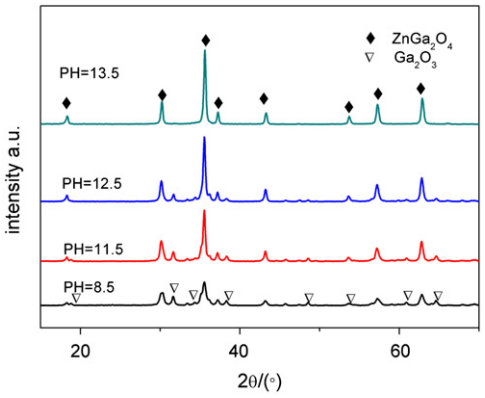

Fig. 1. XRD patterns of $ZnGa_2O_4$ crystallites prepared at different pH values under the hydrothermal temperature of 170 °C.

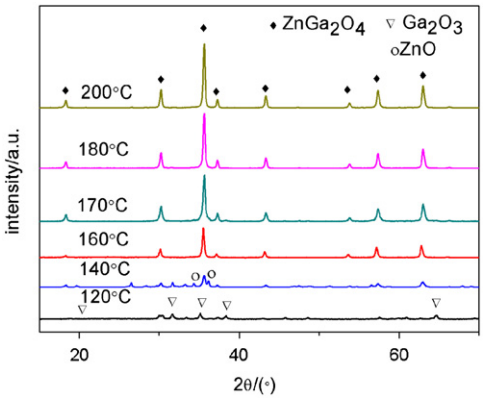

Fig. 2. The XRD patterns of the as-prepared $ZnGa_2O_4$ crystallites at different hydrothermal temperatures when the pH value is 13.5.

3. Results and discussion

3.1. The influence of pH value on the phase of the crystallites

Fig. 1 shows the XRD patterns of $ZnGa_2O_4$ crystallites prepared at different pH values under the hydrothermal temperature of 170 °C. The diffraction lines of $ZnGa_2O_4$ synthesized at pH of 8.5–13.5 and the peak intensity increase with the increase of pH value. However, small diffraction peaks of Ga_2O_3 can be observed in the pH value of 8.5–12.5, which indicates high pH value (>13.5) is beneficial to achieve pure monophase of $ZnGa_2O_4$ crystallites.

3.2. The influence of temperature on the phase and microstructure of the crystallites

The XRD patterns of the as-prepared $ZnGa_2O_4$ crystallites at different hydrothermal temperatures are shown in Fig. 2. It can be seen that the samples prepared at the temperature of 120 °C are composed of Ga_2O_3 phase, and when the temperature is 140 °C, $ZnGa_2O_4$, ZnO, Ga_2O_3 phases are detected in the samples. When the hydrothermal

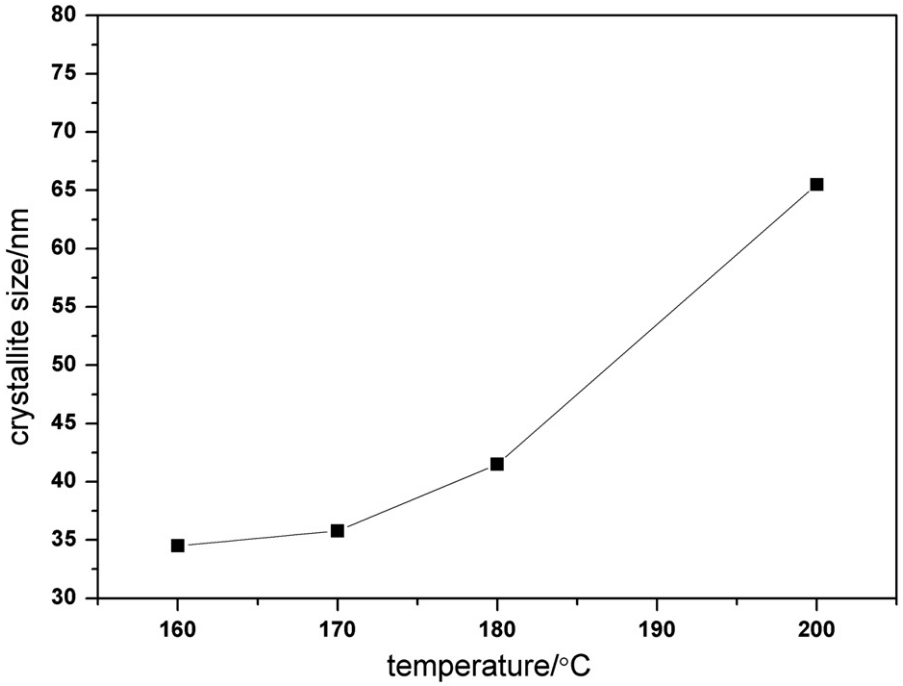

Fig. 3. Effect of hydrothermal treatment temperature on the crystallite size of the $ZnGa_2O_4$ synthesized at the pH value of 13.5.

temperature reaches to 160 °C, monphase of $ZnGa_2O_4$ crystallites can be achieved. Moreover, with the continuous increase of hydrothermal temperature from 170 °C to 200 °C, the increase in peak intensity of $ZnGa_2O_4$ phase is obvious. According to the Scherrer equation [8], the sizes of the synthesized $ZnGa_2O_4$ crystallites are calculated to find grow larger when increasing hydrothermal temperatures (Fig. 3).

Fig. 4 shows the SEM and TEM images of $ZnGa_2O_4$ crystallites obtained at different hydrothermal temperatures at the pH value of 13.5. As is shown in Fig. 4(a), the $ZnGa_2O_4$ crystallites prepared at 160 °C is made up of nano-spheric particles with slight agglomeration. Fig. 4(b) and (c) is the TEM images of $ZnGa_2O_4$ crystallites prepared at 160 °C. From Fig. 4(b), it can be clearly found that the $ZnGa_2O_4$ spheric particles are single crystal and the spacing between adjacent lattice planes is (1 1 1) 0.478 nm (Fig. 4(c)), with the exposed lattice plane being [1 1 1]. Figs. 4(d), (e) and (f) show the SEM images of $ZnGa_2O_4$ crystallites prepared at 170 °C, 180 °C and 200 °C, respectively. Fig. 4(d) shows that the small particles are aggregated to form a cuboid-like morphology. In Fig. 4(e) and (f), with the increase of hydrothermal temperature, the bigger size and denser surface are observed, which may result from the higher pressure of the environment and higher diffusion rate of the ions [11].

3.3. Formation mechanism of $ZnGa_2O_4$ crystallites

From the above XRD, SEM and TEM analyses of $ZnGa_2O_4$ crystallites, it is suggested the possible reactions may happen, as is shown in Eqs. (1–4).

$$Zn^{2+} + 4OH^- = Zn(OH)_4^{2-} \quad (1)$$

$$Ga_2O_3 + 3H_2O = Ga(OH)_3 \quad (2)$$

$$Ga(OH)_3 + OH^- = Ga(OH)_4^- \quad (3)$$

$$Zn(OH)_4^{2-} + 2Ga(OH)_4^- = ZnGa_2O_4 + 4H_2O + 4OH^- \quad (4)$$

In the synthesis process, Zn^{2+} ions and Ga_2O_3 reacted with OH^-, which formed $Zn(OH)_4^{2-}$ and $Ga(OH)_4^-$, respectively. Then the $Zn(OH)_4^{2-}$ and $Ga(OH)_4^-$ formed the $ZnGa_2O_4$ nuclei. When the pH value increases, the phase of Ga_2O_3 reduces and the phase of ZnO cannot be detected. According to the previous report [7,11,12], $Zn(OH)_4^{2-}$ is thought to be more easily formed than $Ga(OH)_4^-$ at the hydrothermal temperature from 100 °C to 200 °C. So we can propose that the OH^- ions play very important role in the preparation of $ZnGa_2O_4$ crystallites. The Zn^{2+} ions react with OH^- first, and then the Ga_2O_3 react with the remainder of OH^- ions. Therefore, the $ZnGa_2O_4$ nucleation rate is controlled by reaction (3).

As the temperature increases to 170 °C, 180 °C and 200 °C, the reaction process is similar to that of 160 °C. However, the morphology of $ZnGa_2O_4$ crystallites alters from spheric particles to a cuboid-like morphology. This may be due to the quantity of $Zn(OH)_4^{2-}$ and $Ga(OH)_4^-$ increasing greatly with the rise of temperature [8]. Subsequently, $ZnGa_2O_4$ particles tend to aggregate to form a cuboid-like morphology in order to lower the specific surface area [13,14]. For the morphologies of 170 °C, 180 °C and 200 °C, we think that the nano-spheric $ZnGa_2O_4$ grains have recrystallization and tend to be denser.

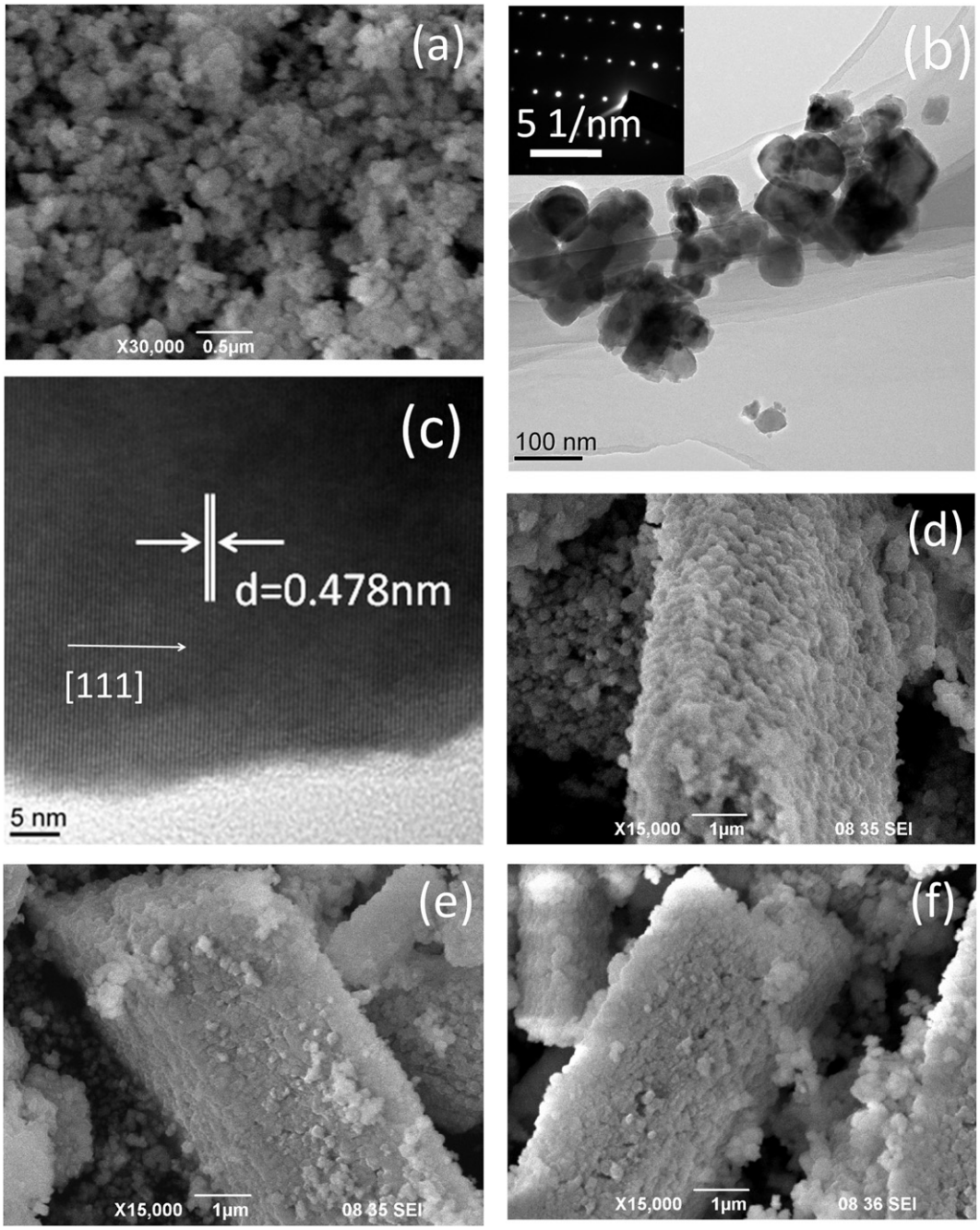

Fig. 4. SEM and TEM images of $ZnGa_2O_4$ crystallites obtained at different hydrothermal temperatures with the pH value of 13.5. (a) SEM picture of $ZnGa_2O_4$ crystallites obtained at 160 °C, (b) TEM picture of $ZnGa_2O_4$ powders obtained at 160 °C. The inset is the SAED pattern form individual $ZnGa_2O_4$ spheric particles: (c) the HRTEM picture of $ZnGa_2O_4$ crystallites obtained at 160 °C, (d)–(f) SEM picture of $ZnGa_2O_4$ crystallites obtained at 170 °C, 180 °C and 200 °C.

3.4. Photocatalytic activity of $ZnGa_2O_4$ crystallites

The photocatalytic activity of $ZnGa_2O_4$ crystallites was evaluated by measuring the degradation rate of RB under ultraviolet light irradiation. Fig. 5 shows the degradation of RB using $ZnGa_2O_4$ crystallites prepared at different hydrothermal temperatures and Ga_2O_3, ZnO prepared at hydrothermal temperature of 160 °C was also tested for comparison. It is found that $ZnGa_2O_4$ crystallites prepared at 160 °C exhibits high photocatalytic performance with 98.4% RB at 60 min, much better than these of Ga_2O_3, ZnO, which demonstrates that not the presence of these phases in the sample synthesized at 160 °C contribute to degradation of RB. When observing Fig. 5, we can draw a conclusion that the photocatalytic degradation of RB follows a pseudo-first-order reaction and its expression [15] is as follows:

$$\frac{dc}{dt} = -K_c C \text{ or } C(t) = C_0 e^{-K_c t} \quad (1)$$

$$\mathrm{In}\left(C_0/C_t\right) = K_c t \quad (2)$$

where K_c is the rate constant. C_0 and C_t represent initial equilibrium concentration of RB and the reaction concentration of RB, respectively.

Then we can get straight lines using regression fitting techniques, and their slopes correspond to the pseudo-first-order rate constant (K_c), as shown in Fig. 6. The calculated K_c, the corresponding pseudo-first-order kinetic equation and the R^2 values are summarized in Table 1. Because of high value of R^2, it demonstrates the pseudo-first-order kinetic equation fits the photocatalytic degradation of RB perfectly.

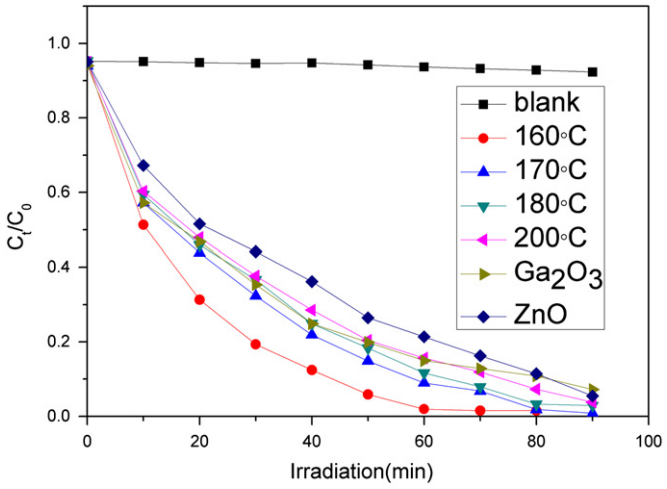

Fig. 5. The photocatalytic degradation curve of the $ZnGa_2O_4$ catalysts at different hydrothermal temperatures and Ga_2O_3, ZnO catalysts at hydrothermal temperature of 160 °C.

Results show that the pseudo-first-order rate constant (K_c) decreases with increase in temperature. Obviously, the photodegradation efficiency of $ZnGa_2O_4$ crystallites decreases with the increase of hydrothermal temperature from 160 °C to 200 °C, and the best photodegradation efficiency is found to be on the sample prepared at 160 °C with the rate constant (K_c) of 0.06885 min^{-1}. Because of high value of R^2, it demonstrates the pseudo-first-order kinetic equation fit the photocatalytic degradation of RB perfectly.

As we know, semiconductor nanoparticles have a higher photocatalytic activity than the bulk materials due to the high surface area and quantum effects. Moreover, the micron sized semiconductor grains cannot efficiently transfer the light-generated charge carriers to the surface and many of them are even lost because of recombination [16,17]. However, nanoparticles can dramatically avoid

Table 1
Parameter and linear kinetic equation of photocatalytic reaction.

Initial concentration C_0 (mg/L)	Temperature	K	Pseudo-first-order kinetic equation	R^2
10	160 °C	0.06885	$\ln(C_0/C_t)=0.06885t-0.5994$	0.94903
	170 °C	0.06148	$\ln(C_0/C_t)=0.06148t-0.5636$	0.93148
	180 °C	0.04769	$\ln(C_0/C_t)=0.04769t-0.2471$	0.95519
	200 °C	0.03927	$\ln(C_0/C_t)=0.03927t-0.0983$	0.96162

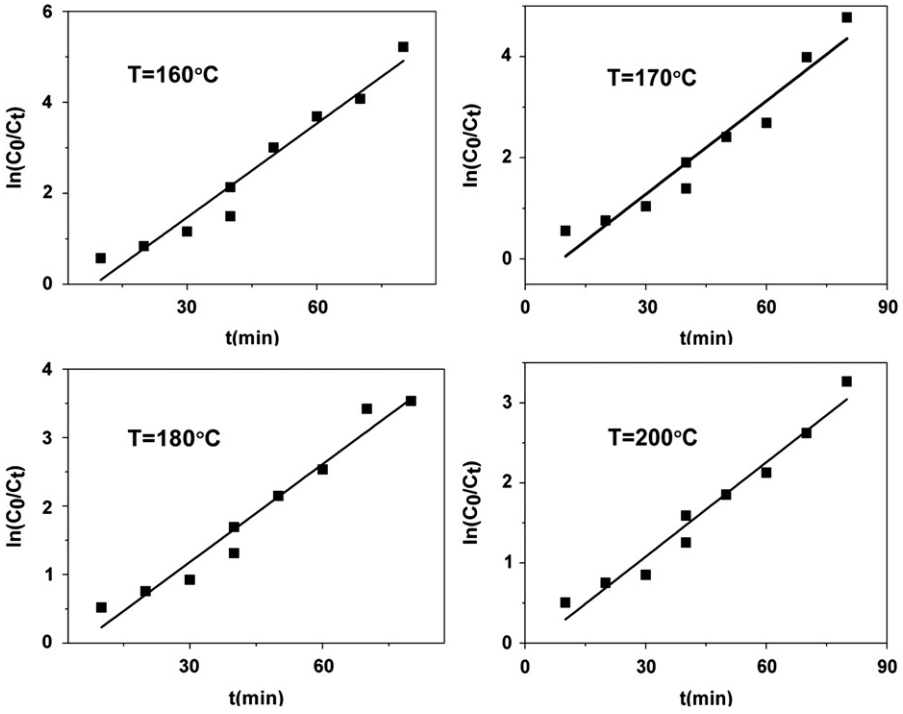

Fig. 6. Relationship between $\ln(C_0/C_t)$ and UV irradiation time of $ZnGa_2O_4$ at hydrothermal temperature of 160 °C, 170 °C, 180 °C and 200 °C.

Table 2
Specific photocatalytic activities of $ZnGa_2O_4$ crystallites in degradation of RB.

Temperature (°C)	BET ($m^2\ g^{-1}$)	Conversion rate ($\mu mol\ g^{-1}\ min^{-1}$)	Areal activity ($\mu mol\ m^{-2}\ min^{-1} \times 10^{-3}$)
160	24.1	0.169	7.01
170	13.4	0.153	11.42
180	11.2	0.141	12.59
200	8.6	0.136	15.81

Note: conversion rate: *n* (Rhodamine B) per gram (catalyst) per hour; areal activity: conversion rate per BET.

those problems and improve the solar energy conversion efficiency compared to the micron sized grains [18].

The specific activities of $ZnGa_2O_4$ crystallites prepared at different hydrothermal are listed in Table 2. Indeed, the $ZnGa_2O_4$ crystallites prepared at 160 °C exhibit the highest BET and Conversion rate. From Fig. 4(a) and (b), we know that the $ZnGa_2O_4$ crystallites prepared at 160 °C have nano-spheric morphology, which answers that they have the best photocatalytic activity. In the temperature range of 170–200 °C, from Table 2, the BET increases and the areal activity decreases, which may be because with the improvement in crystallization and a cuboid-like morphology, the light-generated charge carriers recombination centers will be decreased and thus lead to improvement in photocatalytic activity and decrease in areal activity[19,20]. Therefore, their photocatalytic activities are ranked as follows: 200 °C < 180 °C < 170 °C < 160 °C, and the order of areal activity is inversed.

4. Conclusions

In summary, nano-spheric $ZnGa_2O_4$ particles could be conveniently prepared by hydrothermal method. It was found that the pH value and hydrothermal temperatures were the crucial factors determining the preparation of $ZnGa_2O_4$ particles, and their morphologies could be controlled via adjusting the hydrothermal temperatures. The growth mechanisms of $ZnGa_2O_4$ particles were proposed and it was found that the nuclei reaction rate of $ZnGa_2O_4$ particles was controlled by the formation of $Ga(OH)_4^-$. From the degradation of RB, we could find that their photocatalytic activity was in the order of 200 °C < 180 °C < 170 °C < 160 °C, and the order of areal activity is inversed possibly due to the improvement in crystallization and a cuboid-like morphology.

Acknowledgments

The authors acknowledge the support of the Natural Science Foundation of Shaanxi province(2010JM6001) and Natural Science Foundation of Shaanxi Educational office (2010JK444). The authors would like to thank Mr. Wu for helping with the XRD measurements and Miss Yao for helping with the English presentation, both grammar and it style.

References

[1] I. Ahmad Md, M. Kottaisamy, N. Rama, M.S. Ramachandra Rao, S.S. Bhattacharya, Thin film luminescence of $ZnGa_2O_4$: Mn deposited by PLD, Scripta Materialia 54 (2006) 237–240.
[2] X. Chen, H. Xue, Z. Li, L. Wu, X. Wang, X. Fu, Ternary wide band gap p-Block metal semiconductor $ZnGa_2O_4$ for photocatalytic benzene degradation, Journal of Physical Chemistry C 112 (2008) 20393–20397.
[3] M. Cao, I. Djerdj, M. Antonietti, M. Niederberger, Nonaqueous synthesis of colloidal $ZnGa_2O_4$ nanocrystallites and their photoluminescence properties, Chemistry of Materials 19 (2007) 5830–5832.
[4] H. Xue, Z. Li, L. Wu, Z. Ding, X. Wang, X. Fu, Nanocrystallitesline ternary wide band gap p-block metal semiconductor $Sr_2Sb_2O_7$: hydrothermal syntheses and photocatalytic benzene degradation, Journal of Physical Chemistry C 112 (2008) 5850–5855.
[5] X. Sun, K. Maeda, M. Le Faucheur, K. Teramura, K. Domen, Preparation of $(Ga_{1-x}Zn_x)$ $(N_{1-x}O_x)$ solid-solution from $ZnGa_2O_4$ and ZnO as a photo-catalyst for overall water splitting under visible light, Applied Catalysis A: General 327 (2007) 114–121.
[6] L. Zou, X. Xiang, M. Wei, F. Li, D.G. Evans, Single-crystallitesline $ZnGa_2O_4$ spinel phosphor via a single-source inorganic precursor route, Inorganic Chemistry 47 (2008) 1361–1369.
[7] M. Hirano, Hydrothermal synthesis and characterization of $ZnGa_2O_4$ spinel fine particles, Journal of Materials Chemistry 10 (2000) 469–472.
[8] M. Hirano, M. Imai, M. Inagaki, Preparation of $ZnGa_2O_4$ spinel fine particles by the hydrothermal method, Journal of the American Ceramic Society 83 (2000) 977–979.
[9] M. Hirano, N. Sakaida, Hydrothermal synthesis and low-temperature sintering of zinc gallate spinel fine particles, Journal of the American Ceramic Society 85 (2002) 1145–1150.
[10] W. Zhang, J. Zhang, Z. Chen, T. Wang, Photocatalytic degradation of methylene blue by $ZnGa_2O_4$ thin films, Catalysis Communications 10 (2009) 1781–1785.
[11] H. Xue, Z. Li, Z. Ding, L. Wu, X. Wang, X. Fu, Hollow rods of nanocrystalline $NiGa_2O_4$: hydrothermal synthesis, formation mechanism, and application in photocatalysis, Crystal Growth & Design 8 (2008) 4511–4516.
[12] T.H. Le, Q.D. Truong, T. Kimura, H. Li, C. Guo, S. Yin, T. Sato, Y.-C. Ling, Synthesis of hierarchical porous ZnO microspheres and its photocatalytic deNO*x* activity, Ceramics International 38 (2012) 5053–5059.
[13] Y. Li, X. Duan, H. Liao, Y. Qian, Self-regulation synthesis of nanocrystallitesline $ZnGa_2O_4$ by hydrothermal reaction, Chemistry of Materials 10 (1998) 17–18.
[14] G.-J. Xing, R. Liu, C. Zhao, Y.-L. Li, Y. Wang, G.-M. Wu, Photoluminescence and photocatalytic properties of uniform $PbMoO_4$ polyhedral crystals synthesized by microemulsion-based solvothermal method, Ceramics International 37 (2011) 2951–2956.
[15] S.L. Li, Y.P. Zhou, J.J. Liu, Physical Chemistry, third ed., Higher Education Press, Tianjin, 2009.
[16] L. Xu, Y. Su, Q. Zhou, S. Li, Y. Chen, Y. Feng, Self-assembled catalyst growth and optical properties of single-crystallitesline $ZnGa_2O_4$ nanowires, Crystallites Growth & Design 7 (2007) 810–814.

[17] H. Xue, Z. Li, Z. Ding, L. Wu, X. Wang, X. Fu, Hollow rods of nanocrystallitesline $NiGa_2O_4$: hydrothermal synthesis, formation mechanism, and application in photocatalysis, Crystallites Growth & Design 8 (2008) 4511–4516.
[18] J. Xie, Y. Li, W. Zhao, L. Bian, Y. Wei, Simple fabrication and photocatalytic activity of ZnO particles with different morphologies, Powder Technology 207 (2011) 140–144.
[19] X. Zhang, J. Huang, K. Ding, Y. Hou, X. Wang, X. Fu, Photocatalytic decomposition of benzene by porous nanocrystallitesline $ZnGa_2O_4$ with a high surface area, Environmental Science & Technology 43 (2009) 5947–5951.
[20] H. Tian, J. Ma, K. Li, J. Li, Hydrothermal synthesis of S-doped TiO_2 nanoparticles and their photocatalytic ability for degradation of methyl orange, Ceramics International 35 (2009) 1289–1292.